Astronomy & Astrophysics manuscript no. mblanco_rn3
April 10, 2014
©ESO 2014

arXiv:1404.2333v1 [astro-ph.SR] 8 Apr 2014

CRIRES-VLT high-resolution spectro-astrometry as a tool in the search of small structures at the cores of Planetary Nebulae ⋆ *(Research Note)*

M.W. Blanco Cárdenas[1], H.U. Käufl[2], M.A. Guerrero[1], L.F. Miranda[3,4], and A. Seifahrt[5]

[1] Instituto de Astrofísica de Andalucía (IAA-CSIC), Glorieta de la Astronomía s/n, 18008 Spain
e-mail: mblanco@iaa.es, mar@iaa.es
[2] European Southern Observatory (ESO), Karl Schwarzschild Str. 2 D-85748 Garching bei München, Germany
e-mail: hukaufl@iaa.es
[3] Universidad de Vigo, Departamento de Física Aplicada, Facultad de Ciencias, Campus Lagoas-Marcosende s/n, 36310 Vigo, Spain
e-mail: lfm@iaa.es
[4] Consejo Superior de Investigaciones Científicas (CSIC), C/ Serrano 117, E-28006, Madrid, Spain
[5] Department of Astronomy and Astrophysics, University of Chicago, Chicago, IL 60637, USA
e-mail: seifahrt@oddjob.uchicago.edu

Received September 15, 1996; accepted March 16, 1997

ABSTRACT

The onset of the asymmetry in planetary nebulae (PNe) occurs during the short transition between the end of the asymptotic giant branch (AGB) phase and the beginning of the PN phase. Sources in this transition phase are compact and emit intensely in infrared wavelengths, making high spatial resolution observations in the infrared mandatory to investigate the shaping process of PNe. Interferometric VLTI IR observations have revealed compelling evidence of disks at the cores of PNe, but the limited sensitivity, strong observational constraints, and limited spatial coverage place severe limits on the universal use of this technique. Inspired by the successful detection of proto-planetary disks using spectro-astrometric observations, we apply here for the first time this technique to search for sub-arcsecond structures in PNe. Our exploratory study using CRIRES (CRyogenic high-resolution Infra-Red EchelleSpectrograph) commissioning data of the proto-PN IRAS 17516−2525 and the young PN SwSt 1 has revealed small-sized structures after the spectro-astrometric analysis of the two sources. In IRAS 17516−2525, the spectro-astrometric signal has a size of only 12 mas, as detected in the Brγ line, whereas the structures found in SwSt 1 have sizes of 230 mas in the [Fe III] line and 130 mas in the Brγ line. The spectroscopic observations required to perform spectro-astrometry of sources in the transition towards the PN phase are less time consuming and much more sensitive than VLTI IR observations. The results presented here open a new window in the search of the small-sized collimating agents that shape the complex morphologies of extremely axisymmetric PNe.

Key words. techniques: spectroscopic – high-resolution, ISM: jets and outflows – planetary nebulae: general – planetary nebulae: individual: IRAS 17516−2525, SwSt 1

1. Planetary nebulae: shapes, shaping and observational challenges

Planetary nebulae (PNe) emerge after the asymptotic giant branch (AGB) phase of low- and intermediate-mass stars ($0.8M_{\odot} < M_i < 8M_{\odot}$). PNe display an exceptional variety of morphologies whose shaping involves dramatic changes in the otherwise round envelopes of their progenitors. The most axisymmetric PNe represent a challenge to the understanding of their formation, since they confront the canonical Generalized Interacting Stellar Wind model (GISW, Balick & Frank 2002) . These PNe are believed to be sculpted by fast collimated outflows (jets), whose collimation and launch would be produced by strong magnetic fields (García-Segura et al. 2005) and/or binary systems (Soker 1998). De Marco (2009) proposed the association of disks with the binary evolution through a common-envelope phase.

As revealed by multiwavelength observations in the mid-IR and radio (Sahai et al. 2007), the onset of the asymmetry in PNe occurs during the short transition between the end of the AGB phase and the beginning of the PN phase, when they are optically obscured. IR observations have revealed asymmetries in post-AGB sources and early proto-PNe such as bipolar lobes, and pinched waists and bright cores that appear as dark lanes at optical wavelengths (Suárez et al. 2009, 2011; Verhoelst et al. 2009; Lagadec et al. 2011; Blanco et al. 2013). Meanwhile, radio and mid-IR spectroscopic and interferometric observations have found strong evidences of small-sized dust and/or gaseous disks at the core of a few proto-PNe and young PNe. Bujarrabal et al. (2005) found a Keplerian disk of 900 mas in size at the **centre** of AFGL 915, whereas disks ∼30 mas have been detected by MIDI-VLTI in M 2-9 and Mz 3 (Chesneau et al. 2007; Lykou et al. 2011) and a disk of 40 mas traced by water maser emission has been found in radio observations of the core of young PNe K 3-35 (Miranda et al. 2001; Uscanga et al. 2008).

These results illustrate the need for high-resolution IR and radio observations. MIDI-VLTI and AMBER-VLTI have achieved superb spatial resolutions, but these interferometric ob-

⋆ Based on observations collected at the European Organisation for Astronomical Research in the Southern Hemisphere, Chile. Commissioning: 60.A-9051(A)

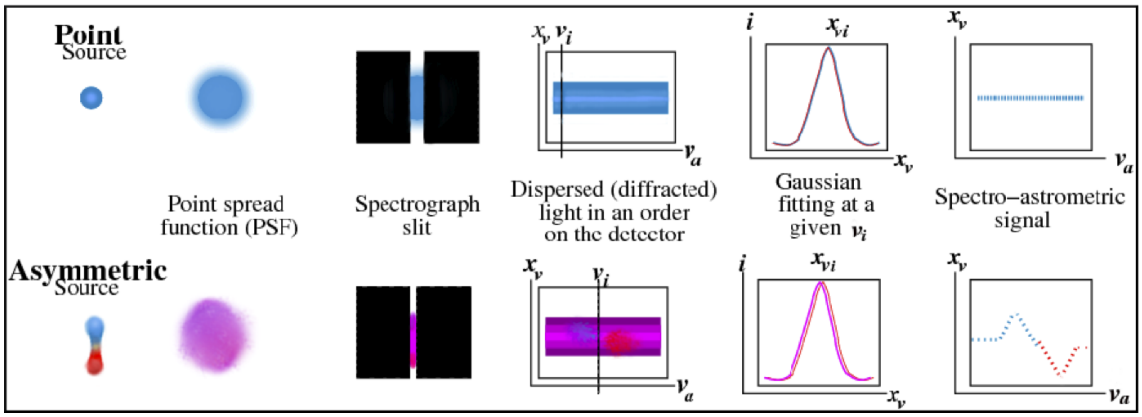

Fig. 1. Sketch of the SA technique (adapted from Whelan & Garcia 2008) showing the analysis of the long-slit spectra of a point source (*top*) and a compact bipolar PN (*bottom*). The major axis of the bipolar PN is assumed to be tilted with respect to the observer, with a lobe approaching (blue) and the other receding (red). The observation conditions smear out both sources into objects resembling unresolved point sources (magenta for the bipolar PN). The SA signal does not reveal any offset for the true point source, but those are unveiled for the bipolar PNe after the SA analysis. In the latter, an antisymmetric SA signature arises because the velocity shifts of the approaching and receding lobes are correlated with their location at both sides of the adjacent central star continuum.

servations are challenging and time consuming. Furthermore, the interpretation of the few available baselines, which are not always suitably aligned with the orientation of the source on the sky, is strongly dependent on models. Finally, the sensitivity of these observations is limited.

An alternative to overcome the difficulties of VLTI observations is the use of high-resolution spectro-astrometric (SA) studies. This observational technique has proven its efficiency in the search for close binaries (Bailey 1998; Takami et al. 2001), disks around B[e] stars (Oudmaijer et al. 2008), jets launched by brown dwarfs (Whelan et al. 2005), and protoplanetary disks (Pontoppidan et al. 2008, 2011). In the latter, Keplerian disks traced by the CO rovibrational fundamental band at 4.7 μm with sizes in the range of 60–180 mas (Pontoppidan et al. 2008) have been detected using CRIRES-VLT (Käufl et al. 2004). This instrumental setup overcomes previous attempts to use this technique with optical data that lacks the spatial resolution to unveil small-sized nebular components (e.g. HM Sagittae nova and the young PNe Vy 2-2, Solf 1984; Miranda & Solf 1991). As compared to spectro-astrometry at optical wavelengths the IR observations are less affected by extinction. The resolved scales suggest rather compact objects, hence being less sensitive to local extinction. This fact maybe a decisive advantage of IR spectro-astrometry, when it comes to reconstruct source geometries from the spectro-astrometric signatures. Therefore, CRIRES high-resolution SA observations can open a new window in the search of compact structures in which high spatial resolution is crucial.

In this work we explore the SA capabilities of CRIRES for the detection and analysis of disk-like structures and small-scale asymmetrical features in objects in their transition to PNe. In Sect. 2 we describe the SA technique at high-resolution and the CRIRES commissioning observations used in this exploratory program. Preliminary results are described in Sect. 3 and a short summary is presented in Sect. 4

2. CRIRES high-resolution spectro-astrometry

The SA technique takes advantage of high-resolution spectral observations to recover spatial details at mas scales by adopting the stellar continuum adjacent to a spectral feature as an astrometric reference. By using a low order adaptive optics module, CRIRES allows to push further the spatial resolution limit while rejecting artifacts which have been reported from the applications of the SA technique to seeing limited data. The SA technique is very attractive because it can be used to retrieve spatial information on scales that normally require interferometric observations, but using a single telescope with a standard instrumental setup.

The use of the SA technique is illustrated in Figure 1 for a point source (a star) and a compact bipolar PN with its major axis tilted with respect to the observer. Both sources are blurred by the diffraction of the telescope, optical imperfections of the system, and residual seeing, and appear unresolved according to the Rayleigh criterion, but the information of small-sized bipolar lobes is embedded within the dispersed spectrum. The SA analysis can trace the centroid of the signal along the spatial axis (x_v) of the 2-dimensional spectrum as a function of the radial velocity (v_i). The accuracy to trace this centroid will depend on the S/N, which determines the PSF fitting precision. The centroid at each velocity is determined by fitting a Gaussian function to the spatial intensity profile as such a function is a reasonable approximation to the point spread function (PSF) along the spatial direction of a dispersed spectrum (Stone 1989). Once the centroid at a certain velocity (x_{v_i}) is computed for all velocities in the wavelength range (v_a) of interest, the variations of the spatial position of the centroid as a function of the velocity can be traced without the dilution provoked by diffraction, optical imperfections, and seeing.

The true spatial offset of a line may be more extended than measured due to drag induced induced to its centroid by the continuum emission. The drag depends on the relative intensities of line and continuum. In this work we have adopted Pontoppidan et al. (2008)'s formulation to derive and correct these effects on the SA signature, such that the corrected offset is computed as:

$$\Delta X_{vi} = \Delta x_{vi} \times (1 + F_c(v)/F_l(v)) \quad (1)$$

where ΔX_{vi} is the corrected offset, Δx_{vi} is the offset measured by the Gaussian fitting, and F_c and F_l are the continuum and line fluxes, respectively. We will refer to ΔX_{vi} as the SA signature.

When the signal-to-noise ratio in the spectrum is sufficient, the original spatial structure will produce a SA signature. This signature will vary with the slit orientation: a physical structure tilted with respect to the plane of the sky and aligned along the

slit will result in maximal SA signature, but minimal or no signature if oriented across the slit. A true point source will show a SA signature with no spatial offsets, independently of the orientation of the slit on the sky. On the contrary, a bipolar PN will show an antisymmetric SA signature because it has spectral signatures (the emission line from the approaching and receding lobes) correlated with spatial coordinates.

The SA technique can reveal spatial structures with angular sizes down to small fractions of a pixel, on scales typically as small as 1/100th of the telescope diffraction pattern. We recall, however, that this technique does not produce direct images of a source; only after a spatio-kinematical modeling of several slit positions, a given source geometry can be favored. In those cases when there is not enough information, the spatio-kinematical modeling may result in solutions that are not unique.

3. Observations, data reduction, and analysis

We have used CRIRES commissioning data to search for mas structures in sources in their transition towards the PN phase. CRIRES operates in the near IR, from 1 to 5 μm, offering the possibility to study ionized and molecular material, as well as the dust features already present in the near-IR L-band. CRIRES can reach a spectral resolution of ∼100,000 when the 0.″2 slit width and the adaptive optic (AO) module are used.

The proto-PN IRAS 17516−2525 and the young PN SwSt 1 were observed on June 11, 2006, and June 5, 2006, respectively. The observations were taken with the AO loop closed and the 0.″2 slit width. The slit was oriented along a PA of 0°, and two nodding positions were used, with exposure times of 120 s. The observational template AutoNodOnSlit with a small nodding throw ∼10″, commonly used for compact sources, was used for IRAS 17516−2525. The observational template Generic with a large nodding throw >25″, ideal for extended sources, was used for SwSt 1. The data were registered by a 4×1 mosaic of Raytheon 1024×1024 pixel InSb Aladin III detectors with pixel size of 27 μm. The detector readout mode was FowlerNsamp. The observations covered the spectral range 2.115–2.168 μm.

The data were reduced using standard IRAF procedures for long-slit spectra. Self developed IDL programs were used to complete the necessary corrections. The combined spectra were corrected for telluric absorptions using the spectro-photometric standard stars HR 5985 for IRAS 17516−2525 and HR 7933 for SwSt 1. The spatial resolution before the SA analysis, as derived from the full width at half maximum ($FWHM$) of the stellar continuum, was 0.″44 for the Brγ line of IRAS 17516−2525, and 0.″70 and 0.″66 for the Brγ and [Fe III] lines of SwSt 1. We note that CRIRES was not optimally focused during this first commissioning run.

The combined spectra used for SA analyses were corrected from detector misalignment at mas scales that might affect the signatures obtained by fitting the continuum position using a second order polynomial fit in the case of SwSt 1 and a third order polynomial fit for IRAS 17516-2525. The centroid along the slit (spatial) direction was derived at each wavelength around lines of interest by fitting a Gaussian profile to the spatial intensity profile obtained in small apertures of 2×60 pixel^2 ≡ 3 km s^{-1}× 5.″16. Additional IDL programs were written to perform the SA analysis. It is important to mention that, even though the observations here presented were not specifically tailored to this purpose, they have allowed us to develop the methodology and programing tools to apply the SA technique to search for mas structures in proto-PNe and young PNe.

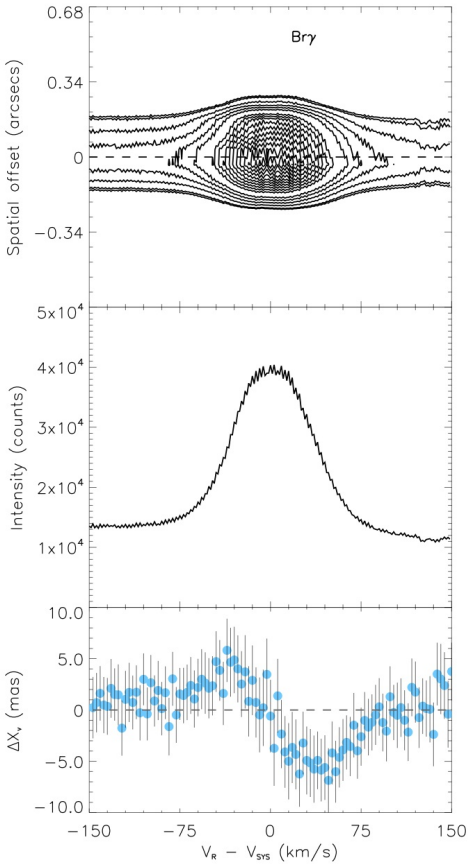

Fig. 2. PV map (*top*), line profile (*middle*), and SA signature (*bottom*) of the Brγ λ2.160 μm line of IRAS 17516−2525.

4. Spectro-astrometric preliminary results

IRAS 17516−2525 has been classified as a proto-PN, although its morphology has not been revealed yet; the source appears compact in near-IR images (1″ in size, Ramos-Larios et al. 2009, 2012) and it is not resolved in the mid-IR imaging catalogue of post-AGB stars presented by Lagadec et al. (2011), despite the nearly-diffracted angular resolution of these images. The spectroscopic study of Sánchez-Contreras et al. (2008) found a P-Cygni profile in the Hα line, but the Pa lines do not show this profile. We have selected the Br$\gamma\lambda$2.160 μm line detected in the CRIRES (Figure 2) spectrum to carry out the SA analysis. A preliminary inspection reveals that the line profile appears broad and single peaked. The SA analysis shows a compact antisymmetric position-velocity (PV) pattern extending ∼12 mas in size (ΔV ∼80 km s^{-1}). Although this SA signature is reminiscent of those interpreted by Pontoppidan et al. (2008) as protoplanetary disks, a disk rotating at this speed would require a gravitational potential unfeasible for a proto-PN. Small-sized bipolar lobes arising from the central regions of this source provide a more likely interpretation for this SA signature.

SwSt 1 is a compact PN with a C-rich central star. Spectroscopic studies have found P-Cygni profiles in the C III λ4650 Å and C IV λ5801 Å lines, but these are not present in the Hα, Hβ, and Hδ lines (De Marco et al. 2001). The morphology of SwSt 1 is not fully resolved in *HST* images (De Marco et al. 2001), but they suggest the presence of a compact, ∼2″ toroidal structure elongated in the east-west direction. In near IR K-band (Likkel et al. 2006) and far-UV (Sterling et al. 2005) observa-

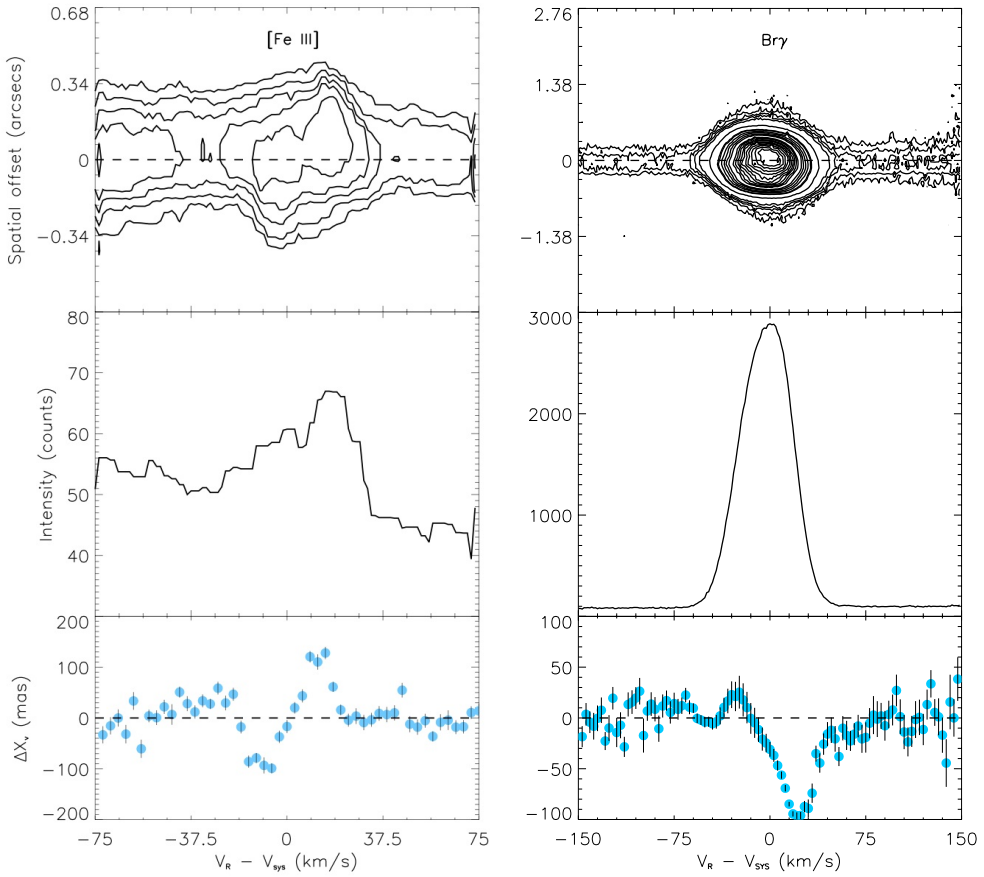

Fig. 3. PV map (*top*), line profile (*middle*), and SA signature (*bottom*) of the [Fe III] λ2.14 μm (*left*) and Brγ λ2.160 μm (*right*) lines of SwSt 1. The SA signal for the two lines are basically reversed, suggesting that they trace different nebular components.

tions, SwSt 1 shows high iron abundances and inhomogeneities in the dust-to-gas ratio across the nebula.

The PV plots of the [Fe III] λ2.145 μm and Brγ λ2.160 μm (Figure 3) show certain asymmetry, particularly the [Fe III] line. The SA analysis reveals antisymmetric PV features ∼230 mas in size ($\Delta V \approx$22 km s^{-1}) in the [Fe III] line and ∼130 mas in size in the Brγ line ($\Delta V \approx$50 km s^{-1}). Besides the different sizes, there is an obvious change in the shape and orientation of the signatures. This is reminiscent of sources in which distinct structural components with varying physical conditions are traced by different emission lines, such as the young PN Hb 12 (Welch et al. 1999) and the proto-PN CRL 2688 (Sahai et al. 1998). We can argue that in SwSt 1 the [Fe III] line (IP=30.7 eV) arises from a region in the nebula close to its central star, where the higher density and temperature of the material enhances its emissivity (Bautista & Pradhan 1998; Zhang et al. 2012), whereas the location of the Brγ line (IP=13.6 eV) emitting region is less constrained.

5. Summary

Using long-slit high-resolution spectra, the SA technique enables us to resolve small-sized structures in different astronomical objects. Inspired by these results, we have investigated the use of this technique in the search of structures at mas scales at the innermost regions of sources in the transition from the AGB to the PN phase. For this purpose, we have used CRIRES commissioning data of the proto-PN IRAS 17516−2525 and the young PN SwSt 1 to develop the methodology and the tools to perform such SA analyses.

Our SA analysis has been able to detect the presence of a small-sized structure, ∼12 mas in size, in IRAS 17516−2525 that can be interpreted as small bipolar lobes. As for SwSt 1, the SA analysis shows two structures with different sizes, ∼130-230 mas, and inclinations in the [Fe III] and Brγ lines. Tailored SA observations at different PAs with its corresponding calibrations, as well as a proper model fitting, are mandatory to derive a conclusive interpretation of the SA signatures.

Remarkably, the SA analysis based on CRIRES commissioning data has been able to detect structures which are comparable in size to those resolved by MIDI-VLTI in Mz 3 and M 2-9, and more compact than those detected in AFGL 915 with radio-interferometric observations at Plateau de Bure. Compared to MIDI-VLTI, CRIRES SA observations are more sensitive, not restricted by fixed baselines, and the data interpretation is less model dependent. We conclude that the SA technique is very suitable for the search of small-sized disks and asymmetric structures in the short transition from the AGB to the PN phase.

Acknowledgements. MWBC and MAG are supported by the Spanish MICINN (Ministerio de Ciencia e Innovación) grant AYA 2011-29754-C03-02, and LFM by grant AYA 2011-30228-C03-01, both co-funded with FEDER funds. MWBC would like to thank the EEBB-FPI for the grant for the short term stay in 2012, and thank the European Southern Observatory (ESO) Headquarters in Garching, Germany, for all the facilities provided during her stay. We thank Dr. X. Fang for helpful discussion on the excitation of the [Fe III] λ2.14 μm in PNe.

References

Bailey, J. 1998, MNRAS, 301, 161
Balick, B., & Frank, A. 2002, ARA&A, 40, 439, hep-ph/9609357

Bautista, M. A., & Pradhan, A. K. 1998, ApJ, 492, 650, hep-ph/9609357
Blanco Cárdenas, M. W., Guerrero, M. A., Ramos-Larios, G., et al. 2013, A&A, 551, A64, hep-ph/9609357
Bujarrabal, V., Castro-Carrizo, A., Alcolea, J., & Neri, R. 2005, A&A, 441, 1031, hep-ph/9609357
Chesneau, O., Lykou, F., Balick, B., et al. 2007, arXiv:0710.0499, hep-ph/9609357
Coffey, D., Bacciotti, F., Podio, L., & Nisini, B. 2010, ApJ, 719, 505, hep-ph/9609357
De Marco, O., Crowther, P. A., Barlow, M. J., Clayton, G. C., & de Koter, A. 2001, MNRAS, 328, 527, hep-ph/9609357
De Marco, O. 2009, PASP, 121, 316, hep-ph/9609357
García-Segura, G., López, J. A., & Franco, J. 2005, ApJ, 618, 919, hep-ph/9609357
Kaeufl, H.-U., Ballester, P., Biereichel, P., et al. 2004, Proc. SPIE, 5492, 1218, hep-ph/9609357
Lagadec, E., Verhoelst, T., Mékarnia, D., et al. 2011, MNRAS, 417, 32, hep-ph/9609357
Likkel, L., Dinerstein, H. L., Lester, D. F., Kindt, A., & Bartig, K. 2006, AJ, 131, 1515, hep-ph/9609357
Lykou, F., Chesneau, O., Zijlstra, A. A., et al. 2011, A&A, 527, A105, hep-ph/9609357
Miranda, L. F., & Solf, J. 1991, A&A, 252, 331, hep-ph/9609357
Miranda, L. F., Gómez, Y., Anglada, G., & Torrelles, J. M. 2001, Nature, 414, 284, hep-ph/9609357
Oudmaijer, R. D., Parr, A. M., Baines, D., & Porter, J. M. 2008, A&A, 489, 627, hep-ph/9609357
Pontoppidan, K. M., Blake, G. A., van Dishoeck, E. F., et al. 2008, ApJ, 684, 1323, hep-ph/9609357
Pontoppidan, K. M., Blake, G. A., & Smette, A. 2011, ApJ, 733, 84, hep-ph/9609357
Ramos-Larios, G., Guerrero, M. A., Suárez, O., Miranda, L. F., & Gómez, J. F. 2009, A&A, 501, 1207, hep-ph/9609357
Ramos-Larios, G., Guerrero, M. A., Suárez, O., Miranda, L. F., & Gómez, J. F. 2012, A&A, 545, A20, hep-ph/9609357
Sahai, R., Hines, D. C., Kastner, J. H., et al. 1998, ApJ, 492, L163, hep-ph/9609357
Sahai, R., Morris, M., Sánchez Contreras, C., & Claussen, M. 2007, AJ, 134, 2200, hep-ph/9609357
Sánchez Contreras, C., Sahai, R., Gil de Paz, A., & Goodrich, R. 2008, ApJS, 179, 166, hep-ph/9609357
Soker, N. 1998, MNRAS, 299, 1242, hep-ph/9609357
Solf, J. 1984, A&A, 139, 296, hep-ph/9609357
Sterling, N. C., Dinerstein, H. L., Bowers, C. W., & Redfield, S. 2005, ApJ, 625, 368, hep-ph/9609357
Stone, R. C. 1989, AJ, 97, 1227 , hep-ph/9609357
Suárez, O., Gómez, J. F., Miranda, L. F., et al. 2009, A&A, 505, 217, hep-ph/9609357
Suárez, O., Lagadec, E., Bendjoya, P., et al. 2011, Asymmetric Planetary Nebulae 5 Conference, 7P, hep-ph/9609357
Takami, M., Bailey, J., Gledhill, T. M., Chrysostomou, A., & Hough, J. H. 2001, MNRAS, 323, 177, hep-ph/9609357
Uscanga, L., Gómez, Y., Raga, A. C., et al. 2008, MNRAS, 390, 1127, hep-ph/9609357
Verhoelst, T., Waters, L. B. F. M., Verhoeff, A., et al. 2009, A&A, 503, 837, hep-ph/9609357
Whelan, E. T., Ray, T. P., Bacciotti, F., et al. 2005, Nature, 435, 652, hep-ph/9609357
Whelan, E., & Garcia, P. 2008, Jets from Young Stars II, 742, 123, hep-ph/9609357
Welch, C. A., Frank, A., Pipher, J. L., Forrest, W. J., & Woodward, C. E. 1999, ApJ, 522, L69, hep-ph/9609357
Zhang, Y., Fang, X., Chau, W., et al. 2012, ApJ, 754, 28, hep-ph/9609357